

# **DESIGN AND SIMULATION OF FUZZY LOGIC CONTROL SYSTEM FOR ROBOTIC TWO-LINK MANIPULATORS**

**Mr. N. Selvagesan, Mr. Prabhu Jude. R, Dr. S.Renganathan, Mr. S.Magesh**

**Department of Instrumentation, Madras Institute of Technology, Chennai – 600 044.**

## **ABSTRACT**

Robotic manipulators are subjected to both structured and unstructured uncertainties even in a well-structured setting. This paper attempts to design a fuzzy logic controller for controlling the position of the arms of a two-link manipulators taking into account the disturbances caused by inertial loading, coupling reaction forces between joints (Coriolis and centrifugal), and gravity loading effects. The design for the position control incorporates a torque computation block that compensates for the disturbances caused by these effects and a fuzzy logic controller. The simulation results for the position control of a two-link robotic manipulator using the compensated fuzzy logic model were then compared with the results obtained using an optimized PID controller. The results clearly indicated that the performance of the compensated fuzzy logic controller was much better than the optimized PID controller even for nonlinear disturbances.

# **DESIGN AND SIMULATION OF FUZZY LOGIC CONTROL SYSTEM FOR ROBOTIC TWO-LINK MANIPULATORS**

**Mr. N. Selvagesan, Mr. Prabhu Jude. R, Dr. S.Renganathan, Mr. S.Magesh**

**Department of Instrumentation, Madras Institute of Technology, Chennai – 600 044.**

## **1. Introduction**

The robotic manipulators are highly coupled, nonlinear and time-varying systems that are generally subjected to both structured and unstructured uncertainties. This makes the accurate position control of the robotic arms a very complicated and difficult engineering problem. With the use of the robots in the medical and sensitive industrial applications gaining popularity, the precision position control of the robot arms has turned into an inevitable requirement. This demand for the accurate position control calls for a method that compensates by and large for the adverse effects of the uncertainties on the positioning of the robot arms. The inertia, gravity and Coriolis Effect have been identified as the major contributors for the inaccuracy in the positioning of the robot arms. Hence an accurate controller invariably has to overcome these adverse effects by including some kind of compensation logic in the design.

## **2. Robot Dynamics**

Robot dynamics basically deals with mathematical formulations of the equations of robot arm motion. The dynamic equations of motion of a manipulator are a set of mathematical equations describing the dynamic behavior of the manipulator. Such equations of motion are useful for computer simulation of the robot arm motion, design of suitable control equations of a robot arm and evaluation of kinematic design and structure of a robot arm. The actual dynamic model can be obtained from known physical laws such as the laws of Newtonian and Lagrangian mechanics.

### 3. L-E Formulation

The general motion equations of a manipulator can conveniently be expressed through the direct application of the Lagrange Euler (L-E) formulation to non - conservative systems. The L-E equation is given as follows

$$d / dt (\partial L / \partial \dot{q}_i) - \partial L / \partial q_i = \tau_i \quad i = 1,2,3,\dots,n$$

where

L = Lagrangian function = kinetic energy K- potential energy P

K = total kinetic energy of the robot arm

P = total potential energy of the robot arm

$q_i$  = generalized coordinates of the robot arm

$\dot{q}_i$  = first time derivative of the generalized coordinate,  $q_i$

$\tau_i$  = generalized force (or torque) applied to the system at joint i to drive link i

From the above Lagrange-Euler equation, one is required to properly choose a set of generalized coordinates to describe the system. Generalized coordinates are used as a convenient set of coordinates that completely describe the location (position and orientation) of a system with respect to a reference coordinate frame. For a simple manipulator with rotary-prismatic joints, various sets of generalized positions of the joints are readily available because they can be measured by potentiometers or encoders or other sensing devices, they provide a natural correspondence with the generalized coordinates. Thus, in the case of a rotary joint,  $q_i \equiv \theta_i$ , the joint angle span of the joint.

### 4. Motion Equations of a manipulator

The derivation of equations of motion of a manipulator requires the computation of the total kinetic energy and the total potential energy of the manipulator.

#### 4.1 Kinetic Energy of the manipulator

If  $dK_i$  is the kinetic energy of a particle with differential mass  $dm$  in link i; then

$$\begin{aligned} dK_i &= \frac{1}{2}(\dot{x}_i^2 + \dot{y}_i^2 + \dot{z}_i^2) dm \\ &= \frac{1}{2} \text{trace} (\dot{v}_i \dot{v}_i^T) dm \end{aligned}$$

$$= \frac{1}{2} \text{Tr} (v_i v_i^T) dm$$

where  $v_i = \left( \sum_j U_{ij} q_j \right) {}^i r_i$        $j$  varies from 1 to  $i$

$$U_{ij} = \begin{cases} {}^0 A_{j-1} Q_j {}^{j-1} A_i & \text{for } j \leq i \\ 0 & \text{for } j > i \end{cases}$$

$Q_j$  is a 4 x 4 matrix, given as [ (0 -1 0 0), (1 0 0 0), (0 0 0 0), (0 0 0 0)] for revolute joint. ... (1)

${}^i r_i$  = fixed point at rest in a link 'i' w.r.t homogeneous coordinates of the  $i^{\text{th}}$  link coordinate

${}^i A_j$  = homogeneous coordinate transformation matrix which relates  $j^{\text{th}}$  coordinate frame to the  $i^{\text{th}}$  coordinate frame.

The total kinetic energy of all the links can be found out by integrating  $dK_i$  over all the links.

The total kinetic energy  $K$  of a robot arm after integration will be found as

$$K = \int dK_i = \frac{1}{2} \text{Tr} \left[ \sum_p \sum_r U_{ip} (J_i) U_{ir}^T q_p q_r \right] \quad p, r \text{ varies from } 1 \text{ to } i \quad \dots\dots(2)$$

where

$J_i$  is the inertia of all the points on link  $i$  given by

$$J_i = \int {}^i r_i {}^i r_i^T dm$$

## 4.2 Potential Energy of the Manipulator

Let  $P_i$  be the  $i^{\text{th}}$  link's potential energy. The  $P_i$  is given by

$$P_i = -m_i g ({}^0 A_i {}^i \check{r}_i) \quad i = 1, 2, \dots\dots\dots n$$

where  ${}^0 A_i$  is the coordinate transformation matrix which relates the  $i^{\text{th}}$  coordinate frame to the base coordination frame

${}^i \check{r}_i$  is the a fixed point in the  $i^{\text{th}}$  link expressed in homogenous coordinates with respect to the  $i^{\text{th}}$  link coordinate frame .

The total potential energy  $P$  of the robot manipulator is found out by integrating  $P_i$  over all the links.

$$P = \sum_i P_i = \sum_i -m_i g ({}^0A_i \check{r}_i) \quad i \text{ varies from } 1 \text{ to } n \quad \dots\dots(3)$$

Where  $g = (0, 0, -|g|, 0)$  and  $g$  is the gravitational constant. ( $g = 9.8062 \text{ m/sec}^2$ )

### 4.3 L-E formulation for the two-link manipulator

From equations (2) and (3), the Lagrangian function  $L = K-P$  is given by

$$L = \frac{1}{2} \sum_i \sum_j \sum_k [ \text{Tr} (U_{ij} J_i U_{ik}^T) \dot{q}_i \dot{q}_k ] + \sum_i m_i g ({}^0A_i \check{r}_i) \quad i \text{ varies from } 1 \text{ to } n, j, k \text{ varies from } 1 \text{ to } i$$

Applying the Lagrange-Euler formulation to the Lagrangian function, the generalized torque for joint  $i$  actuator to drive the  $i^{\text{th}}$  link of the manipulator,

$$\tau_i = \sum_j \sum_k \text{Tr} (U_{jk} J_j U_{ji}^T) \dot{q}_k \ddot{q}_j + \sum_j \sum_k \sum_m \text{Tr} (U_{jkm} J_j U_{ji}^T) \dot{q}_k \dot{q}_m - \sum_j m_j g U_{ji}^j \check{r}_j$$

for  $i = 1, 2, 3, \dots, n$

where  $j$  varies from  $i$  to  $n$ ;  $k$  and  $m$  varies from  $1$  to  $j$

The above equation can be expressed in a much simpler matrix form as

$$\tau(t) = D ( \dot{q}(t) ) \ddot{q}(t) + h(q(t), \dot{q}(t)) + c(q(t))$$

where  $\tau(t) = n \times 1$  generalized torque vector applied at joints  $i = 1, 2, \dots, n$ , that is,

$$\tau(t) = (\tau_1(t), \tau_2(t), \dots, \tau_n(t))^T$$

$q(t) =$  an  $n \times 1$  vector of the joint variables of the robot arm and can be expressed as

$$q(t) = (q_1(t), q_2(t), \dots, q_n(t))^T$$

$\dot{q}(t) =$  an  $n \times 1$  vector of the joint velocity of the robot arm and can be expressed as

$$\dot{q}(t) = (\dot{q}_1(t), \dot{q}_2(t), \dots, \dot{q}_n(t))^T$$

$\ddot{q}(t) =$  an  $n \times 1$  vector of the joint acceleration of the joint variables  $q(t)$  and can be expressed as

$$\ddot{q}(t) = (\ddot{q}_1(t), \ddot{q}_2(t), \dots, \ddot{q}_n(t))^T$$

$D(q)$  = an  $n \times n$  inertial acceleration-related symmetric matrix whose elements are

$$D_{ik} = \sum_j \text{Tr} (U_{jk} J_j U_{ji}^T) \quad i, k = 1, 2, \dots, n$$

$j$  varies from  $\max(i,k)$  to  $n$

$h(q, q')$  = an  $n \times 1$  nonlinear Coriolis and centrifugal force vector whose elements are

$$h(q, q') = (h_1, h_2, \dots, h_n)^T$$

$$\text{Where } h_i = \sum_k \sum_m q_k' q_m' \quad i = 1, 2, \dots, n. \quad \dots(4)$$

$$\text{and } h_{ikm} = \sum_j \text{Tr} (U_{jkm} J_j U_{ji}^T) \quad i, k, m = 1, 2, \dots, n$$

$j$  varies from  $\max(i,k,m)$  to  $n$

$c(q)$  = an  $n \times 1$  gravity loading force vector whose elements are

$$c(q) = (c_1, c_2, \dots, c_n)^T$$

$$\text{Where } c_i = \sum_j (-m_j g U_{ji}^j \ddot{r}_j) \quad i = 1, 2, \dots, n. \quad \dots(5)$$

$j$  varies from  $i$  to  $n$ .

The computational complexity of the L-E formulation increases with the 4<sup>th</sup> power of the number of degrees of freedom of the robot arm. Hence for the simulation purpose a specific simple case of a two-link manipulator with revolute joints is taken. We assume the following in our derivation of the generalized torque equation for the two-link manipulator: joint variables =  $\theta_1, \theta_2$ , mass of the links =  $m_1, m_2$ , link parameters =  $a_1 = a_2 = 0$ ;  $d_1 = d_2 = 0$ ;  $a_1 = a_2 = l$ .

The homogenous coordinate transformation matrices  ${}^{i-1}A_i$  ( $i = 1, 2$ ) are obtained as

$${}^0A_1 = [(C_1, -S_1, 0, lC_1), (S_1, C_1, 0, lS_1), (0, 0, 1, 0), (0, 0, 0, 1)] \quad \dots(6)$$

$${}^1A_2 = [(C_2, -S_2, 0, lC_2), (S_2, C_2, 0, lS_2), (0, 0, 1, 0), (0, 0, 0, 1)] \quad \dots(7)$$

$${}^0A_2 = {}^0A_1 {}^1A_2 = [(C_{12}, -S_{12}, 0, l(C_{12} + C_1)), (S_{12}, C_{12}, 0, l(S_{12} + S_1)), (0, 0, 1, 0), (0, 0, 0, 1)] \quad \dots(8)$$

where  $C_i = \cos \theta_i$ ;  $S_i = \sin \theta_i$ ;  $C_{ij} = \cos (\theta_i + \theta_j)$ ;  $S_{ij} = \sin (\theta_i + \theta_j)$

From the eqns 1, 6, 7, 8 we can derive the following results

### *Inertia Effects:*

The elements of the acceleration related symmetric matrix  $D(\theta)$  can be found as

$$D_{11} = 1/3 m_1 l^2 + 4/3 m_2 l^2 + m_2 C_2 l^2. \quad \dots\dots(9)$$

$$D_{12} = D_{21} = 1/3 m_2 l^2 + 1/2 m_2 C_2 l^2. \quad \dots\dots(10)$$

$$D_{22} = 1/3 m_2 l^2. \quad \dots\dots(11)$$

Where  $D_{11}$ ,  $D_{12}$ ,  $D_{21}$ ,  $D_{22}$  are inertia elements.

### *Coriolis Effects:*

The velocity related coefficients in the Coriolis and Centrifugal terms could be obtained from equations 4 and 5

$$\text{as } h_1 = -1/2 m_2 S_2 l^2 \theta_2'^2 - m_2 S_2 l^2 \theta_1' \theta_2', \quad \dots\dots(12)$$

$$h_2 = -1/2 m_2 S_2 l^2 \theta_1'^2 \quad \dots\dots(13)$$

### *Gravity Effects:*

The gravity loading force vector elements can be obtained from equation 5 as

$$c_1 = 1/2 m_1 g l C_1 + 1/2 m_2 g l C_{12} + m_2 g l C_1 \quad \dots\dots(14)$$

$$c_2 = 1/2 m_2 g l C_{12} \quad \dots\dots(15)$$

Finally, the L-E equations of motion for the two-link manipulator are found to be

$$\tau_1 = 1/3 m_1 l^2 + 4/3 m_2 l^2 + m_2 C_2 l^2 + 1/3 m_2 l^2 + 1/2 m_2 C_2 l^2 - 1/2 m_2 S_2 l^2 \theta_2'^2 - m_2 S_2 l^2 \theta_1' \theta_2' + 1/2 m_1 g l C_1 + 1/2 m_2 g l C_{12} + m_2 g l C_1 \quad \dots\dots(16)$$

$$\tau_2 = 1/3 m_2 l^2 + 1/2 m_2 C_2 l^2 + 1/3 m_2 l^2 - 1/2 m_2 S_2 l^2 \theta_1'^2 + 1/2 m_2 g l C_{12} \quad \dots\dots(17)$$

## **5. Design of the controller**

The Figure 1 shows the block diagram for the position control of two-link manipulator using a fuzzy logic controller without disturbance compensation. The basic design of our controller remains same as given in the Figure 1; however, an additional block for the torque compensation logic (termed C-logic) is added to overcome the structured and unstructured uncertainties. The Figure 2 shows the block diagram of the designed controller with the C-logic block incorporated to the original design.

The design of the individual blocks is summarized below.

### 5.1 C-Logic Block

The C-Logic block shown here can be expressed as a combination of the L-E torque computation block and a torque to voltage converter (T-V converter). The C-Logic block can be delineated as shown in Figure 3. The torque computation block calculates the torque experienced in the joints 1 and 2 from the generalized angular coordinate position of the arms as given by the equations 16 and 17. The torque outputs are then fed to the T-V converter. The T-V converter calculates the voltage that corresponds to a particular combination of torque ( $\tau$ ) and the time derivative of the angular position of the arm ( $\theta$ ) as given by the formula

$$v = \left[ \theta' K_{fb} + (\tau * R_m) / K_{torque} \right] * \text{Gear Ratio}$$

where  $K_{fb}$ =feed back constant

$K_{torque}$ =torque constant

$R_m$ = mechanical resistance

### 5.2 Fuzzy Logic Controller

In our case we designed a fuzzy controller with the error and the first derivative of the error as fuzzy inputs. The error is calculated as the difference between the set point of the arm position and the instantaneous position of the arm. We used the triangular membership function for the fuzzification of the input variables. A 7x7 rule base was designed for each of the two controllers. The output from the inference engine is defuzzified using the center of area methods of defuzzification.

### 5.3 Robot Dynamics Block

This block uses the mechanical and electrical characteristics of the manipulator to convert the voltage input into an equivalent angular position output. The Figure 4 represents the robot dynamics model that we used in our simulation.

## **6. Simulation and Results**

The above-described design was implemented and simulated using MATLAB. The simulation results were then used to compare the performance of the following three different controller configurations

1. An optimized PID controller without disturbance torque compensation
2. Fuzzy logic controller without disturbance torque compensation
3. Fuzzy logic controller with disturbance torque compensation

The performance results are tabulated in Table 2.

The simulation graphs for each of the design are shown in Figures 5, 6 indicating the step response and the sinusoidal response for the controller. The calculated performance indices (as given in table 2) and the simulation results clearly indicate that the performance of the fuzzy logic controller with torque compensation was superior as compared to the controllers of other configurations.

## **7. Conclusion**

This superior performance of the controller is complimented by the reduced oscillations of the control variable about the set point .The figure 7 shows a magnified portion of the simulation graph to demonstrate the amplitude of oscillations experienced by an arm about the set point in the case of optimized PID controllers.

When accurate position control is required for a sensitive industrial or medical application, this kind of oscillations about the set point is highly undesirable.

Hence the proposed design of controller has the following advantages over the conventional controllers:

1. More accurate tracking of the set point variations.
2. Reduced oscillations about the set point
3. Settling time is comparatively smaller.

**Fig 1:** Block Diagram of an uncompensated Fuzzy Logic Controller for the position control of a two-link robotic manipulator.

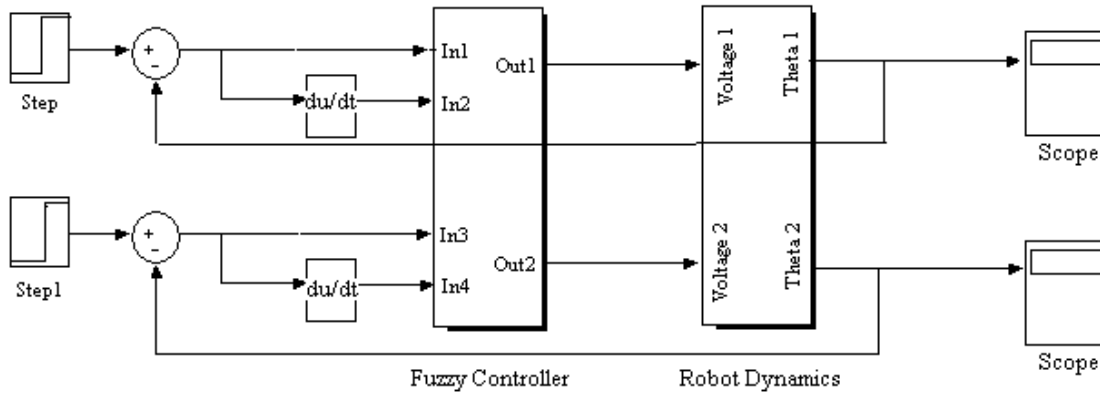


**Fig 2:** Block Diagram of the Compensated Fuzzy Logic Controller for the position control of a two-link robotic manipulator as implemented with SIMULINK.

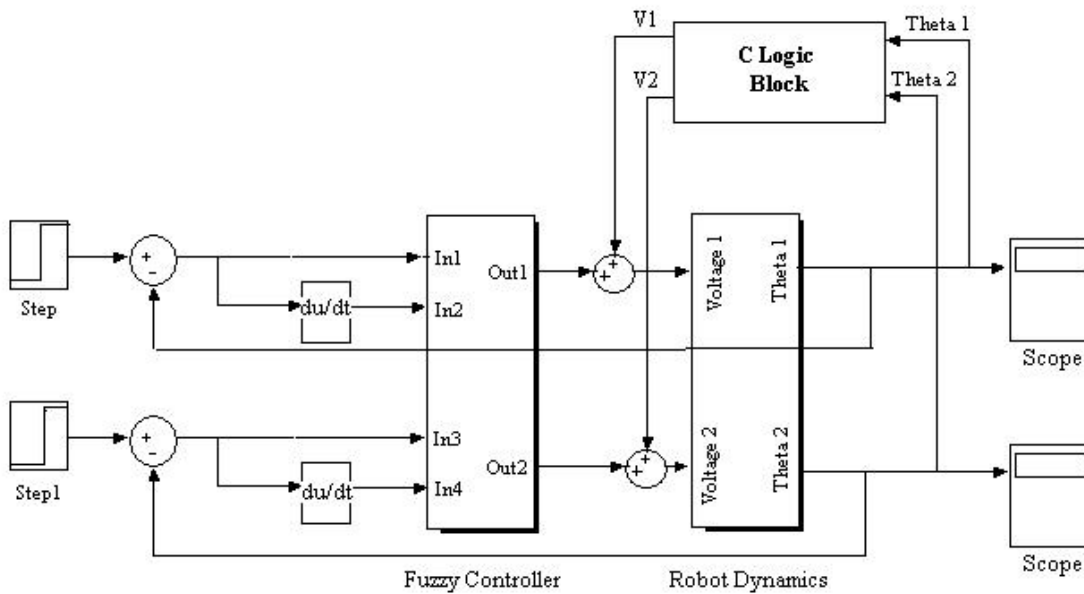


**Fig 3: C-Logic block**

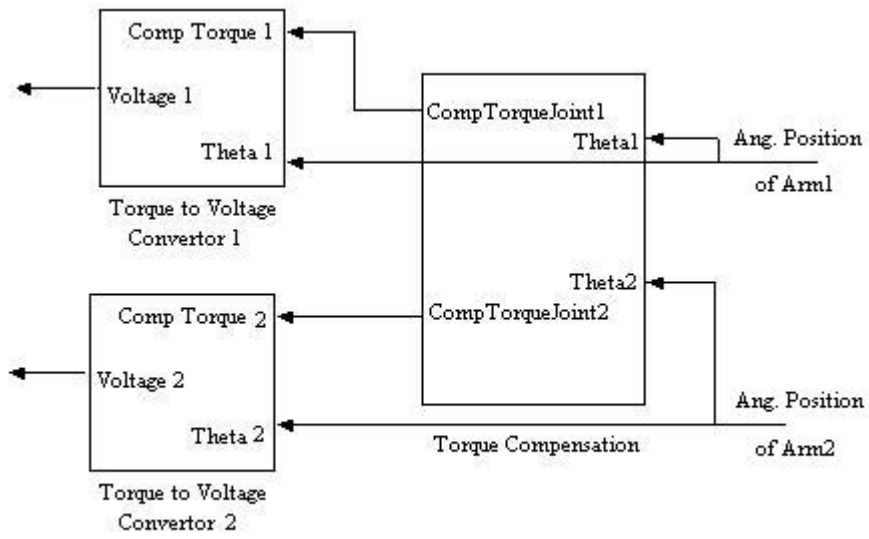


**Fig 4:** Dynamic Model of the Two-link robotic manipulator.

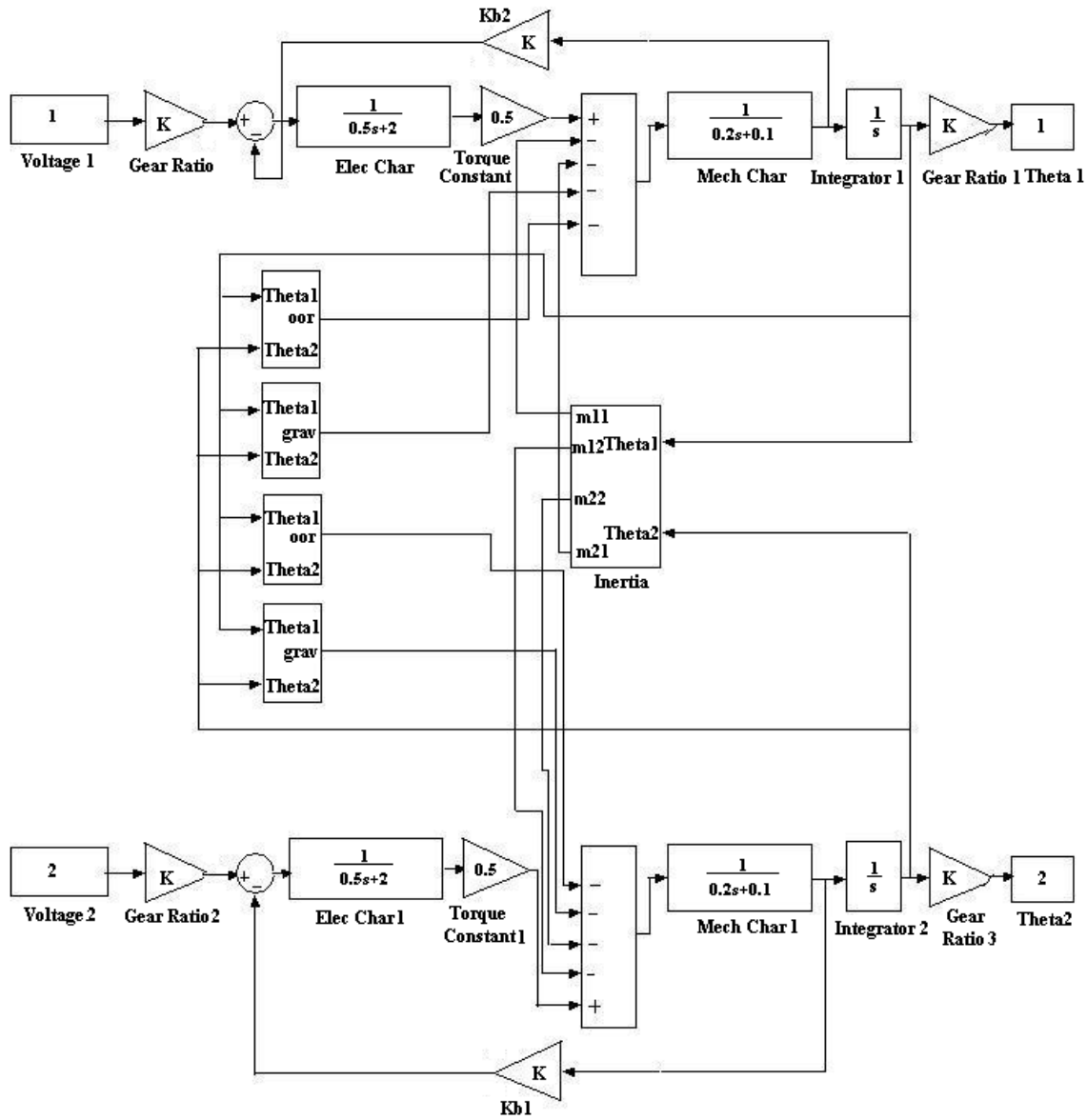


**Fig 5:** Step Response for PID, Uncompensated Fuzzy logic and Compensated Fuzzy Logic Controllers (top to bottom) (Step magnitude=100).

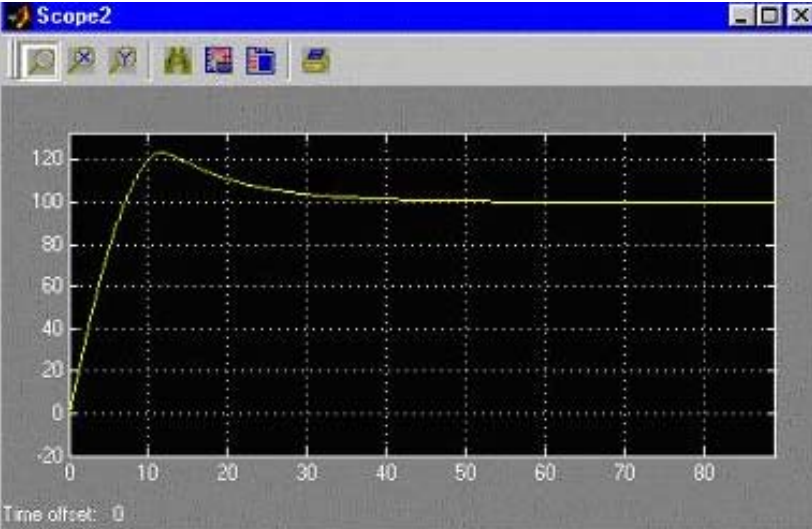
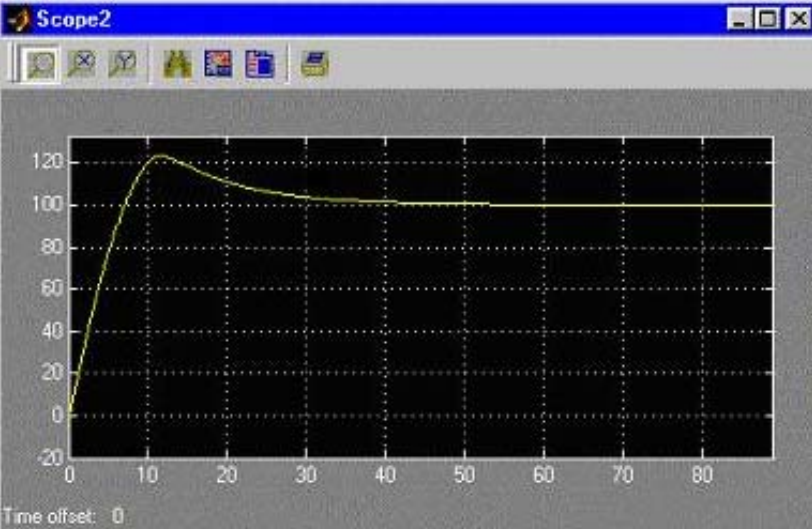
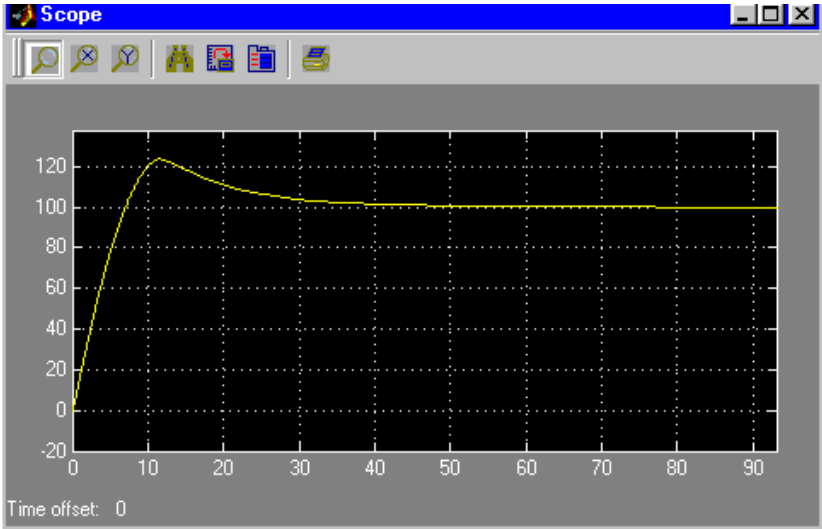


**Fig 6:** Sinusoidal Response for the Compensated fuzzy logic Controller.  
(Sine amplitude =10)

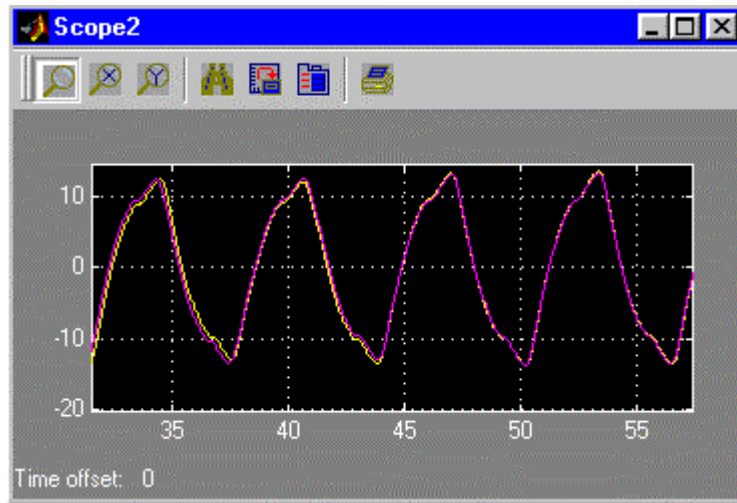


**Fig 7:** Zoomed graph to show the Oscillations about the SP experienced by the arm in the case of PID controller. It can be noted that the Compensated Fuzzy Logic model has a much steady response after the settling time.

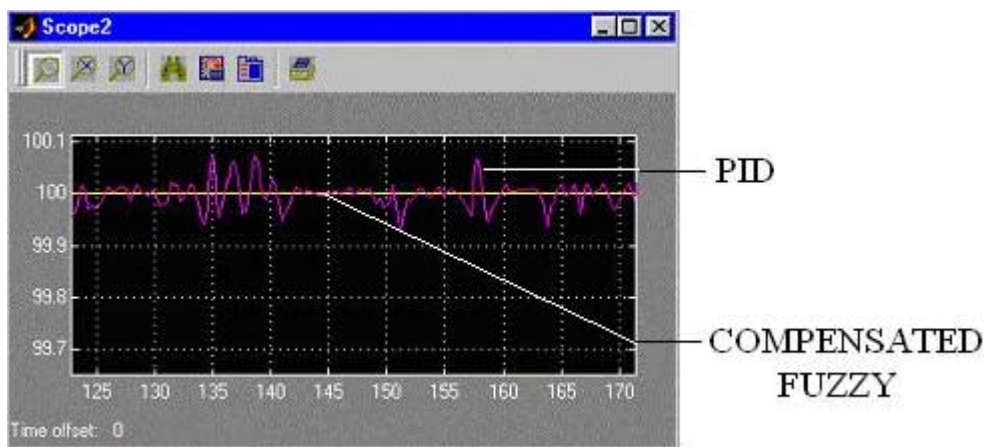


**Fig 8:** Zoomed graph to show the relatively large deviation of the control variable from the SP in the case of Uncompensated fuzzy logic controller as compared with a Compensated Fuzzy Logic model.

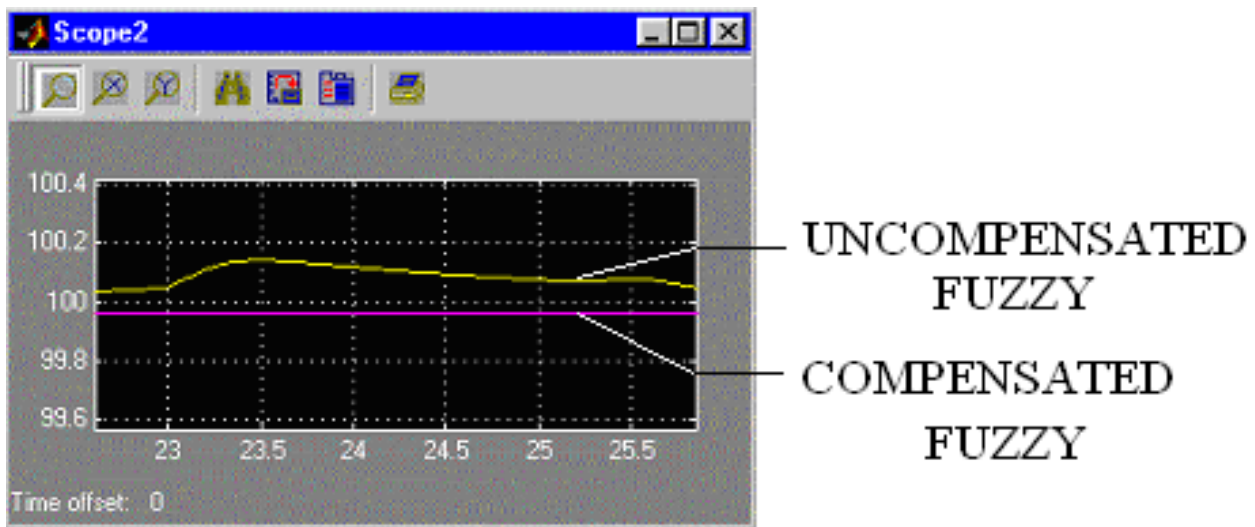


**TABLE 1: INFERENCE TABLE FOR THE FUZZY LOGIC CONTROLLER**

| <b>de/dt<br/>e</b> | <b>NL</b> | <b>NM</b> | <b>NS</b> | <b>Z</b> | <b>PS</b> | <b>PM</b> | <b>PL</b> |
|--------------------|-----------|-----------|-----------|----------|-----------|-----------|-----------|
| <b>NL</b>          | NL        | NL        | NL        | NL       | NM        | NS        | Z         |
| <b>NM</b>          | NL        | NM        | NM        | NM       | NS        | Z         | PS        |
| <b>NS</b>          | NL        | NM        | NS        | NS       | Z         | PS        | PM        |
| <b>Z</b>           | NL        | NM        | NS        | Z        | PS        | PM        | PL        |
| <b>PS</b>          | NM        | NS        | Z         | PS       | PS        | PM        | PL        |
| <b>PM</b>          | NS        | Z         | PS        | PM       | PM        | PM        | PL        |
| <b>PL</b>          | Z         | PS        | PM        | PL       | PL        | PL        | PL        |

**TABLE 2: COMPARISON OF PERFORMANCE INDICES OF COMPENSATED FUZZY LOGIC CONTROLLER WITH PID AND UNCOMPENSATED FUZZY LOGIC CONTROLLER**

| <b>CONTROLLER</b>   | <b>Joint 1</b> |        |        | <b>Joint 2</b> |         |        |
|---------------------|----------------|--------|--------|----------------|---------|--------|
|                     | IAE            | ISE    | ITAE   | IAE            | ISE     | ITAE   |
| PID CONTROLLER      | 7190           | 302513 | 918535 | 3501           | 75628.3 | 459023 |
| UNCOMPENSATED FUZZY | 340.7          | 116138 | 340790 | 290.79         | 84559   | 290790 |
| COMPENSATED FUZZY   | 238.478        | 56872  | 238478 | 188.478        | 35524.1 | 188478 |

The results are taken for a step change in the positional set-point of 100 deg in Joint 1 and 50 deg in Joint 2.

## REFERENCES:

1. R. R. Yager, D. P. Filev, "Essentials of Fuzzy Modeling and Control", New York: Wiley (1994)
2. S. Commuri, F. L. Lewis, "Adaptive-Fuzzy Controllers of Robot manipulators", Int. J. Syst. Sci., vol.27, no.6 (1996)
3. J. J. Craig, "Introduction to Robotics", New York: Addison Wesley (1989)
4. Limin Peng, Peng-Yung Woo, "Neural-Fuzzy Control System for Robotic Manipulators", IEEE Control System Magazine, vol.22, no.1 (2002)
5. K.S.Fu, R.C.Gonzalez, C.S.G.Lee, "Robotics-Control, Sensing, Vision and Intelligence", McGraw Hill Book Company (1987).